Journal of Physics: Conference Series **211** (2010) 012017 doi:10.1088/1742-6596/211/1/012017

Supported and embedded Fe nanoparticles: influence of the environment on shape and interface contributions to the magnetic anisotropy

A Kleibert[1,2], F Bulut[3,4], W Rosellen[3], K H Meiwes-Broer[1], J Bansmann[4] and M Getzlaff[3]

[1] Institute of Physics, University of Rostock, Universitätsplatz 3, D-18051 Rostock, Germany
[2] Swiss Light Source, Paul Scherrer Institute, CH-5232 Villigen, Switzerland
[3] Institute of Applied Physics, University of Düsseldorf, Universitätsstr. 1, D-40225 Düsseldorf, Germany
[4] Institute of Surface Chemistry and Catalysis, Ulm University, Albert-Einstein-Allee 47, D-89069 Ulm, Germany

E-mail: getzlaff@uni-duesseldorf.de

Abstract. A continuously working arc cluster ion source was used to prepare mass-filtered Fe nanoparticles with a mean size of 6 to 10 nm. Their structure was determined by HRTEM. The nanoparticles were deposited into an Al matrix and additionally on a W(110) substrate for comparison. Within the matrix they maintain their spherical shape and do not show any magnetic anisotropic effect. For uncapped Fe nanoparticles on a tungsten surface, a flattening is observed by STM and the nanoparticles exhibit a distinct magnetic anisotropy with the easy magnetization axis being in the surface plane. Correlating both investigations we conclude that this observation is due to shape and interface-induced contributions to the magnetic anisotropy.

1. Introduction

Ferromagnetic nanoparticles with a tunable size of up to 20 nm and a narrow size distribution have attracted considerable interest for future applications ranging from medicine and chemistry to ultrahigh density magnetic storage devices [1]. Many different routes, especially chemistry-based methods suited for large scale applications, have been proposed and partially successfully tested for the production of nanoparticles with desired physical properties [2, 3]. The shape and the crystalline structure of such particles (e.g., [4]) are often influenced by kinetic barriers during the growth process and thus these systems might deviate from thermal equilibrium behavior [5]. As a consequence this class of materials opens the possibility to realize systems with tunable interesting magnetic, structural, and electronic properties. From a technological point of view it is essential to keep in mind that each realistic application requires supported and often embedded nanoparticles in order to guarantee functionality over a sufficiently long time period. However, many studies showed that the particle properties may significantly change when being in contact with a support or a matrix, respectively, particularly when magnetic properties are considered [6]. In order to distinguish pure geometrical (e.g. symmetry) and interface-related effects from additional preparation-induced phenomena it is necessary to investigate the same particles but in different environments. Experimentally, this can be achieved when studying

nanoparticles preformed in the gas phase and subsequently deposited onto different substrates or by codeposition into respective matrices [3, 7–10].

In the present contribution we focus on preformed, mass-filtered Fe nanoparticles being deposited under soft-landing conditions onto (i) a W(110) substrate and (ii) by codeposition into an Al matrix. Combining high resolution transmission electron microscopy (HRTEM), scanning tunneling microscopy (STM), and X-ray magnetic circular dichroism (XMCD) enables us to study the correlation of structure, shape and the magnetic anisotropy [11] in both environments.

2. Experimental details

The Fe particles have been prepared by means of an arc cluster ion source (ACIS) [12]. This source provides mass-filtered pure and alloyed *3d* transition metal nanoparticles with a kinetic energy below 0.1 eV per atom ensuring fragmentation-free deposition conditions [13]. The particle diameters are tuned by applying a dc voltage U_{quad} to an electrostatic quadrupole filter. Using this experimental setup, particles in a size range between 4 and 20 nm are available [14]. XMCD and STM investigations have been carried out *in situ* under UHV conditions (base pressure $< 1 \times 10^{-9}$ mbar). The W(110) crystal was prepared by cycles of heating in oxygen atmosphere and flashing as described in the literature [15, 16]. The surface cleanliness and quality were checked by means of low energy electron diffraction prior to the cluster deposition. In order to avoid agglomeration as well as magnetic dipolar interactions particle ensembles with low density ($<$ 200 nanoparticles per $\mu\mathrm{m}^2$) were prepared in all experiments described here. For the matrix sample first a thick layer of Al was evaporated from a crucible onto a native Si(111) wafer. Subsequently, the Fe particle deposition was started simultaneously to the Al evaporation. Finally, a thick capping layer of Al was prepared to ensure that the particles are fully covered by Al. The XMCD experiments were carried out using circularly polarized synchrotron radiation provided by the PM3 beamline at BESSY (Berlin). Details on the XMCD effect and its applications can be found in the literature [17–19]. Here, magnetization curves were obtained recording the sample drain current (total electron yield detection) with a fixed polarization and the light at an angle of incidence of 30° relative to the surface when applying an external magnetic field in the surface plane and 60° when applying the magnetic field along the perpendicular direction. The photon energy was set to the L_3 edge of Fe. A magnetic field $\vec{B}$ up to 30 mT was applied at variable angle with respect to the sample surface normal allowing to probe anisotropic magnetic properties. For the STM experiment a commercial MicroSTM (Omicron) was used. The probe tips are prepared by chemical etching of a tungsten wire. All measurements were carried out at room temperature in the constant current mode.

3. Results and discussion

3.1. Structure and shape of the Fe particles

Fe particles prepared by the ACIS cluster source have already been characterized in some of our previous studies [14, 20]. Similarly to other experiments a bulk-like bcc lattice in the size range from 6 to about 10 nm was found by means of *ex situ* TEM [21, 22]. The respective particle shape in thermal equilibrium is given by six (001) and twelve (110) surface facets forming a truncated dodecahedron as expected from the Wulff theorem [20, 22, 23]. Two high resolution TEM images are here given as examples in Figs. 1 (a) and (b). The particle in Fig. 1 (a) was deposited onto a carbon-coated TEM grid and subsequently exposed to ambient air for the transport to the microscope. A fourier transform of the image (shown in the inset) reveals a lattice parameter of 0.290 ± 0.005 nm being practically identical with the bulk value of 0.287 nm. After correction for the presence of the native oxide layer we can deduce an initial diameter of the pure metal particle of about 9 nm. We may note that the particle shape in Fig. 1 (a) is largely determined by the oxide shell consisting of irregularly grown oxide grains [24] and thus does not reflect the shape of the pure Fe particle prior to deposition. Fig. 1 (b) shows a particle of similar size but

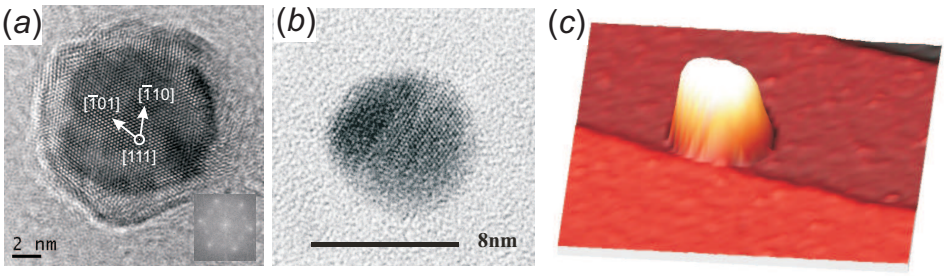

Figure 1. (a) HRTEM image of an Fe nanoparticle deposited on a carbon-coated TEM grid. An oxide shell was formed when exposing the particle to ambient air. A fourier transform of the image (shown in the inset) indicates a bcc lattice with bulk-like lattice parameter of 0.290 ± 0.005 nm in the metallic core. (b) A pure Fe nanoparticle of similar size but embedded in an aluminum matrix. (c) STM image of an individual cluster near a step edge on W(110). The height of the particle amounts to about 7 nm. The image size is 73 nm $\times$ 67 nm and the tunneling parameters are $I = 0.5$ nA, $U = +1.0$ V.

deposited into an Al matrix. As discussed in Ref. [20] the embedded particle is free of oxide and its apparent morphology can be attributed to the above described equilibrium shape.

The actual particle morphology in a deposition experiment may significantly depend on the chosen substrate and on the landing conditions. The equilibrium shape of a supported nanoparticle is in general modified by the interface energy [25]. The high surface energy of W(110) (4 Jm^{-2}) relative to that of Fe (2.4 Jm^{-2}) results in a distinct wetting behavior in respective heteroepitaxy experiments [26, 27]. Accordingly, one may expect that under equilibrium conditions Fe particles are smeared out on W(110) resulting in flat islands of monatomic height as discussed in [28]. However, kinetic barriers can hinder the preformed particles to adopt equilibrium conditions upon deposition. In molecular dynamics simulations it was found that for sufficiently small kinetic and adsorption energy released upon contact to the substrate the initial particle shape can be conserved [13]. Using *in situ* STM we find that under the present conditions the Fe nanoparticles clearly retain a three-dimensional shape upon deposition on W(110) as shown in Fig. 1 (c). Moreover, the particles are randomly distributed on the surface and no signature of diffusion to step edges or surface defects is found (not shown here). Since the lateral dimensions in STM images are affected by convolution effects when tip radius and particles are of comparable size [29, 30] one cannot directly infer the particle morphology from images as given in Fig. 1 (c). However, the particle height can unambiguously be measured [being 7 nm in Fig. 1 (c)] and can be related to the particle diameter determined by means of TEM.

A respective comparison of STM heights and TEM diameters is shown in the upper panel of Fig. 2 for different particle sizes being determined by the setting of U_{quad} in the mass-filtering unit of the ACIS. In each investigation more than 250 particles were measured concerning the diameter and the height, respectively, resulting in an error of about ± 0.5 nm. Obviously, the particles appear partially flattened on the W(110) surface. Thereby, the decrease in the height of the size-selected clusters on W(110) is about 1 nm when compared to the TEM images. A similar flattening has also been found for FeCo alloy clusters on W(110). As discussed in Ref. [31] we ascribe this to thermally activated surface diffusion initiated immediately upon the

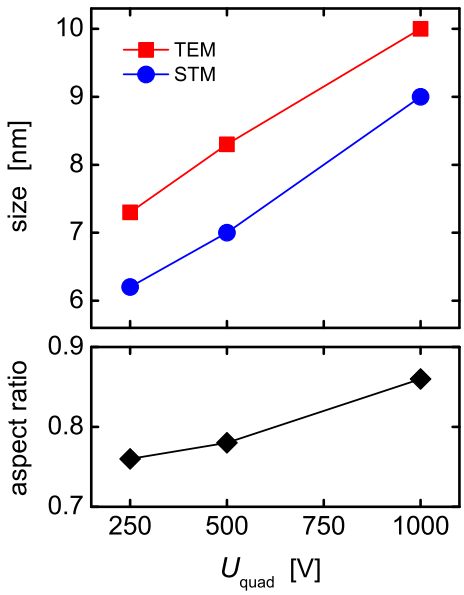

Figure 2. Upper panel: Comparison between the lateral size of size-selected clusters (TEM: red squares) and the height of clusters on W(110) (STM: blue circles) for different cluster sizes. The error amounts to ±0.5 nm. They were produced with variation of the voltages at the electrostatic quadrupole U_{quad}. Lower panel: Corresponding size-dependent aspect ratio. The error amounts to ±0.2.

impact on the substrate, i.e., before the released energy is dissipated. After thermalization no further changes are observed at room temperature and on the time scale of our experiments (a few hours). This also nicely demonstrates how structures far from equilibrium conditions can be achieved and stabilized by deposition of preformed nanoparticles. A detailed discussion concerning the equilibrium shape of crystalline nanoparticles deposited onto a lattice mismatched planar substrate can be found in [32]. Assuming a constant volume before and after deposition and a shape of a spherical cap of the particles in contact with the substrate we can calculate the size-dependent aspect ratio as shown in the lower panel of Fig. 2. The deviation from a spherical shape (aspect ratio = 1) clearly decreases with the particle size. This can also be understood, when considering thermally activated diffusion upon impact. Thereby the length of the diffusion paths being required for an effective material transport increases with the particle size, while the diffusion constant stays constant.

3.2. Magnetic behavior

In situ recorded magnetization curves of Fe nanoparticles on W(110) are significantly affected by the observed shape changes. As shown in Fig. 3 particles deposited with a diameter of about 10 nm are easily magnetized in the surface plane (solid circles), but significantly higher magnetic fields are required for out-of-plane magnetization (open circles). Our data suggest an uniaxial magnetic anisotropy with a hard axis perpendicular to the sample surface. However, the magnetic moments of the particles are not ferromagnetically blocked but thermally fluctuating in the sample plane. The respective magnetization curves can be described by the statistical physics partition function applied to a macrospin as discussed, e.g., in Refs. [33, 34]. The magnetic anisotropy energy of such a sample is then extracted by fitting the partition function to the

datasets. The black lines in Fig. 3 are obtained by a simultaneous fit to both, the in-plane and out-of-plane data and reveal an anisotropy energy of $K = (5.7 \pm 1.7)$ μeV/atom. This value can be compared to calculated shape and interface anisotropy contributions. Based on the observed aspect ratio of about 0.9, respective calculations yield $K_{\mathrm{shape}} = 1.3$ μeV/atom and $K_{\mathrm{interface}} = 6.4$ μeV/atom, cf. Ref. [31], being close to the experimental value. However, the magnitude of the interface term may depend on the orientation of the particles on the W(110) surface. In particular, $K_{\mathrm{interface}}$ might be different for particles resting with their (001) or their (110) facets on the substrate, respectively. As discussed above tip convolution effects prevent us to obtain the orientation of the deposited particles from the STM data. Thus, additional efforts are required to unambiguously determine the origin of the observed anisotropy [35]. Finally, we may note that the fits shown in Fig. 3 are obtained by numerical integration of the partition function. Recently, an analytical expression was derived, which applies when the magnetic field is parallel to the anisotropy axis [36]. This formula might be alternatively used to determine the anisotropy energy from respective data. A further possibility is given by analyzing the initial susceptibility of the magnetization curves with expressions given in Ref. [33].

Magnetization curves were also measured for Fe nanoparticles (with a diameter of 8 nm) embedded in the Al matrix as shown in Fig. 3. The full diamonds (open diamonds) correspond

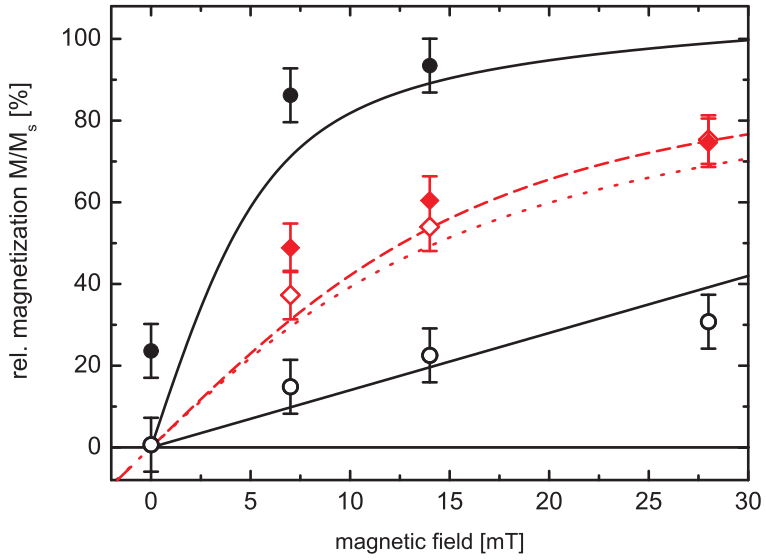

Figure 3. Relative magnetization of 10 nm Fe clusters on W(110) with the magnetic field applied in the surface plane (solid circles) and out-of-plane (open circles) as measured at room temperature. The solid lines are fits to the data as discussed in Ref. [31]. Respective data for 8 nm Fe nanoparticles embedded in an Al matrix with the magnetic field applied in the surface plane (solid diamonds) and out-of-plane (open diamonds). The dashed line depicts a corresponding Langevin curve and the dotted line shows the effect on the magnetization curve when the particles have a relatively weak uniaxial anisotropy with randomly oriented easy axes.

to the magnetization measured with the magnetic field applied parallel (perpendicular) to the sample surface. For this situation there is no evidence for an anisotropic behavior. We may note that the cubic magneto-crystalline anisotropy contribution of bcc Fe amounts to $K_{\mathrm{Fe}} = 3.3$ μeV/atom [37] and the onset of superparamagnetism for particles in the present size range is therefore expected to be far below room temperature (< 25 K [38]). Although the temperature in the present experiments is more than 10 times larger than the blocking temperature, the magnetization curves may still deviate from a respective Langevin curve [36].

To evaluate the effect of the anisotropy we have calculated a Langevin curve given by $M/M_s = coth(NmB/k_BT) - k_BT/NmB$, with m being the magnetic moment per atom, N the number of atoms per particle, k_B the Boltzmann constant, T the temperature, and B the magnitude of the magnetic field. Using $m = 2.2\ \mu_B$ for Fe, $N = 28,000$ corresponding to a particle size of 8 nm, and $T = 290K$ we obtain the dashed curve in Fig. 3 showing a good agreement with the experimental data. For comparison we have computed the magnetization curve of particles with the same size, magnetic moments and at the same temperature, but additionally including the effect of a *uniaxial* anisotropy with randomly distributed easy axes in a respective particle ensemble. Assuming K_{Fe} the statistical partition function yields the dotted curve in Fig. 3 which shows noticeable deviations from the Langevin curve. However, we may note that the magneto-crystalline anisotropy of iron is of *cubic* nature with fourfold symmetry. This may lead to a more Langevin-like behavior of the present particles as suggested by the data in Fig. 3.

Independently of the above discussion, the impact of the environment on the magnetic properties of Fe nanoparticles becomes directly obvious from Fig. 3. The deposition of Fe particles onto a flat W(110) substrate leads to a partial flattening compared to the equilibrium shape. First, this reduces the symmetry of the particle shape. In addition to this the contact interface is different from the remaining particle surface. Both effects lead to an anisotropic magnetic behavior as discussed in detail in Ref. [31]. In contrast, embedding similar particles in an Al matrix retains the high symmetry of the preformed particles as shown in Fig. 1 (b). In fact, the lower surface energy of Al (about 1.1 Jm^{-2} [27]) relative to that of Fe leads to a dewetting behavior thus supporting a spherical particle geometry. As a consequence no shape anisotropy is developed and interface contributions cancel out resulting in an isotropic superparamagnetic behavior.

4. Conclusion

A continuously working arc cluster ion source was used to prepare mass-filtered Fe nanoparticles with sizes ranging from 6 to 10 nm. Their structure was determined by HRTEM. The nanoparticles were deposited on a W(110) substrate and embedded into an Al matrix. In the matrix they maintain their spherical shape, after deposition on a plane substrate without capping a flattening is found by STM, respectively. The magnetic properties were investigated by XMCD. Whereas the deposited nanoparticles exhibit a distinct magnetic anisotropy with the hard magnetization axis being perpendicular to the surface plane the embedded nanoparticles do not show any anisotropic effect. Correlating these investigations we conclude that this observation is due to distinct differences of the respective magnetic shape and interface anisotropy contributions in both systems.

Acknowledgments

We thank J. Carrey (Thomson-CSF, Orsay, France) for TEM investigations, the staff of BESSY for technical assistance, and the DFG for financial support within the priority call 1153 (clusters in contact with surfaces) via DFG BA 1612/3-3, DFG KL 2188/1-3, and DFG GE 1026/4-3.

References

[1] Huber D L 2005 *Small* **1** 482
[2] Sun S H, Murray C B, Weller D, Folks L and Moser A 2000 *Science* **287** 1989
[3] Palmer R E, Pratontep S and Boyen H G 2003 *Nat. Mater.* **2** 443
[4] Antoniak C, Trunova A, Spasova M, Farle M, Wende H, Wilhelm F and Rogalev A 2008 *Phys. Rev. B* **78** 041406
[5] Puntes V F, Krishnan K M and Alivisatos A P 2001 *Science* **291** 2115
[6] Bansmann J *et al.* 2005 *Surf. Sci. Rep.* **56** 189
[7] Bromann K, Felix C, Brune H, Harbich W, Monot R, Buttet J and Kern K 1996 *Science* **274** 956
[8] Getzlaff M, Kleibert A, Methling R, Bansmann J and Meiwes-Broer K H 2004 *Surf. Sci.* **566** 332

[9] Getzlaff M, Bansmann J, Bulut F, Gebhardt R K, Kleibert A and Meiwes-Broer K H 2006 *Appl. Phys.* A **82** 95
[10] Bansmann J, Getzlaff M, Kleibert A, Bulut F, Gebhardt R K and Meiwes-Broer K H 2006 *Appl. Phys.* A **82** 73
[11] Getzlaff M 2008 *Fundamentals of Magnetism* (Berlin Heidelberg: Springer)
[12] Methling R P, Send V, Klinkenberg E D, Diederich T, Tiggesbäumker J, Holzhüter G, Bansmann J and Meiwes-Broer K H 2001 *Eur. Phys. J.* D **16** 173
[13] Haberland H, Insepov Z and Moseler M 2009 *Phys. Rev.* B **79** 125423
[14] Kleibert A, Passig J, Meiwes-Broer K H, Getzlaff M and Bansmann J 2007 *J. Appl. Phys.* **101** 114318
[15] Musket R G, McLean W, Colmenares C A, Makowiecki D M and Siekhaus W J 1982 *Appl. Surf. Sci.* **10** 143
[16] Bode M, Pascal R and Wiesendanger R 1995 *Surf. Sci.* **344** 185
[17] Stöhr J 1999 *J. Magn. Magn. Mat.* **200** 470
[18] Stöhr J and Siegmann H C 2006 *Magnetism* (Berlin Heidelberg: Springer)
[19] Kortright J B, Awschalon D D, Stöhr J, Bader S D, Idzerda Y U, Parkin S S P, Schuller I K and Siegmann H C 1999 *J. Magn. Magn. Mat.* **207** 7
[20] Kleibert A, Meiwes-Broer K H and Bansmann J 2009 *Phys. Rev.* B **79** 125423
[21] Jamet M, Wernsdorfer W, Thirion C, Dupuis V, Mélinon P, Pérez A and Mailly D 2004 *Phys. Rev. B* **69** 024401
[22] Vystavel T, Palasantzas G, Koch S A and De Hosson J T M 2003 *Appl. Phys. Lett.* **82** 197
[23] Wulff G 1901 *Z. Kristallogr.* **34** 449
[24] Fauth K, Goering E, Schütz G and Kuhn L T 2004 *Journal of Applied Physics* **96** 399
[25] Henry C R 2005 *Prog. Surf. Sci.* **80** 92
[26] Gradmann U, Liu G, Elmers H J and Przybylski M 1990 *Hyperfine Interactions* **57** 1845
[27] Vitos L, Ruban A V, Skriver H L and Kollár J 1998 *Surf. Sci.* **411** 186
[28] Reuter D, Gerth G and Kirschner J 1997 *J. Appl. Phys.* **82** 5374
[29] Hoevel H and Barke I 2006 *Prog. Surf. Sci.* **81** 53
[30] Sell K, Kleibert A, von Oeynhausen V and Meiwes-Broer K H 2007 *Eur. Phys. J. D* **45** 433
[31] Kleibert A, Bulut F, Gebhardt R K, Rosellen W, Sudfeld D, Passig J, Bansmann J, Meiwes-Broer K H and Getzlaff M 2008 *J. Phys.: Condens. Matter* **20** 445005
[32] Müller P and Kern R 2000 *Surf. Sci.* **457** 229
[33] Chantrell R, Ayoub N and Popplewell J 1985 *J. Magn. Magn. Mat.* **53** 199
[34] Gambardella P *et al.* 2003 *Science* **300** 1130
[35] Kleibert A, Voitkans A and Meiwes-Broer K H 2009 *submitted*
[36] Fruchart O, Jubert P O, Meyer C, Klaua M, Barthel J and Kirschner J 2002 *J. Magn. Magn. Mat.* **239** 224
[37] Klein H P and Kneller E 1966 *Phys. Rev.* **144** 372–374
[38] Aharoni A 2000 *Introduction to the Theory of Ferromagnetism* (Oxford: Oxford University Press)